Hydrothermal Synthesis and Properties of $Ce_{1-x}Sm_xO_{2-x/2}$ and $Ce_{1-x}Ca_xO_{2-x}$ Solid Solutions

W. Huang, P. Shuk, and M. Greenblatt*

Department of Chemistry, Rutgers, The State University of New Jersey, P.O. Box 939, Piscataway, New Jersey 08855-0939

Received June 13, 1997. Revised Manuscript Received August 12, 1997[⊗]

The structure, thermal expansion coefficients and ionic conductivity of $Ce_{1-x}Sm_xO_{2-x/2}$ and $Ce_{1-x}Ca_xO_{2-x}$ ($x = 0-0.30$) solid electrolytes prepared hydrothermally in a relatively wide concentration range for the first time were systematically investigated. The uniformly small particle size (40−68 nm) of the hydrothermally prepared materials allows sintering of the samples into highly dense ceramic pellets at 1400 °C, a significantly lower temperature, compared to that at 1600 °C required for samples prepared by solid-state techniques. The maximum ionic conductivity was found at $x = 0.17$ for the Sm and at $x = 0.09$ for the Ca-substituted ceria ($\sigma_{600\ °C} = 5.7 \times 10^{-3}$ S/cm, $E_a \approx 0.9$ eV, and $\sigma_{600\ °C} = 2.1 \times 10^{-3}$ S/cm, $E_a \approx 0.8$ eV, respectively). The thermal expansion coefficients, determined from high-temperature X-ray data, are 8.6×10^{-6} and 9.4×10^{-6} K^{-1} for the best conducting $Ce_{0.83}Sm_{0.17}O_{1.915}$ and $Ce_{0.91}Ca_{0.09}O_{1.91}$ solid electrolytes, respectively.

Introduction

In the past several years, CeO_2-based materials have been intensely investigated as catalysts, structural and electronic promoters of heterogeneous catalytic reactions,[1] and oxide ion conducting solid electrolytes in electrochemical cells.[2] The solid electrolyte is a key component of solid-state electrochemical devices, which are increasingly important for applications in energy conversion, chemical processing, sensing, and combustion control.[3−5] For most of these applications, relatively high ionic conductivity of the solid electrolyte is required for device performance. High oxide ion conducting solid electrolytes based on ZrO_2 (zirconia) have been extensively investigated and reviewed in the past.[6−9] Advances in ceramic technology have provided fabrication routes to stabilize the tetragonal phase of zirconia with very good mechanical properties in addition to relatively high oxide ion conductivity.[10] Although yttria-stabilized zirconia is considered to be the most reliable solid electrolyte so far, many studies have been made on other solid electrolytes as alternatives to zirconia, e.g. Bi_2O_3[11−13] and CeO_2[2]-based materials. However, at present, the application of Bi_2O_3-based materials is hindered by their limited electrolytic domain.[13]

Doped ceria is another most promising high-conducting solid electrolyte for solid oxide fuel cell (SOFC) applications. In contrast to pure zirconia, $CeO_{2-\delta}$ has the fluorite structure with oxygen vacancies ($V_O^{\bullet\bullet}$) as the predominant ionic defects:[14−17]

$$2Ce_{Ce}^{\ x} + O_O^{\ x} \rightarrow 2Ce_{Ce}' + V_O^{\bullet\bullet} + {}^1/_2O_2 \qquad (1)$$

where $[Ce_{Ce}^{\ x}] = Ce^{4+}$, $[Ce_{Ce}'] = Ce^{3+}$, and $[O_O^{\ x}]$ is O^{2-} ion on a regular O lattice site.

The oxygen vacancy concentration, and concomitant oxide ion conductivity, in cerium oxide can be increased by the substitution of a lower-valent metal ion for cerium. In the past, many investigations have been carried out on various aspects of ceria solid electrolytes mostly prepared by conventional ceramic methods.[18−30] While the zirconia lattice structure is too small to accommodate a wide range of rare earth dopants, the

* To whom correspondence should be addressed. E-mail: martha@rutchem.rutgers.edu.

[⊗] Abstract published in *Advance ACS Abstracts,* September 15, 1997.

(1) Trovarelli, A. *Catal. Rev.—Sci. Eng.* **1996**, *38*, 439.
(2) Inaba, H.; Tagawa, H. *Solid State Ionics* **1996**, *83*, 1.
(3) Takahashi, T., Kozawa, A., Eds. *Application of Solid Electrolytes*; JEC Press: Ohio, 1980.
(4) Takahashi, T., Ed. *High Conductivity Solid Ionic Conductors*; World Scientific: Singapore, 1989.
(5) Göpel, W., Jones, T. A., Kleitz, M., Lundström, I., Seiyama, T., Eds. *Chemical and Biochemical Sensors*; VCH: Weinheim, Germany, 1991/1992; Vol. 2, 3.
(6) Etsell, T. H.; Flengas, S. N. *Chem. Rev.* **1970**, *70*, 339.
(7) Steele, B. C. H. *Sci. Ceram.* **1980**, *10*, 1.
(8) Subbarao, E.; Maiti, H. S. *Solid State Ionics* **1984**, *11*, 317.
(9) Steele, B. C. H. *J. Power Sources* **1994**, *49*, 1.
(10) Badwal, S. P. S., Ed. *Science and Technology of Zirconia*; Technomic: Lancaster, U.K., 1993.
(11) Takahashi, T.; Iwahara H. *Mater. Res. Bull.* **1978**, *13*, 1447.
(12) Azad, A. M.; Larose, S.; Akbar, S. A. *J. Mater. Sci.* **1994**, *29*, 4135.
(13) Shuk, P.; Wiemhöfer, H.-D.; Guth, U.; Göpel, W.; Greenblatt, M. *Solid State Ionics* **1996**, *89*, 179.
(14) Blumenthal, R. N.; Hofmaier, R. L. *J. Electrochem. Soc.* **1974**, *121*, 126.
(15) Sims, J. R.; Blumenthal, R. N. *High Temp. Sci.* **1976**, *8*, 99.
(16) Tuller, H. L.; Nowick, A. S. *J. Electrochem. Soc.* **1979**, *126*, 209.
(17) Chang, E. K.; Blumenthal, R. N. *J. Solid State Chem.* **1988**, *72*, 330.
(18) Tuller, H. L.; Nowick, A. S. *J. Electrochem. Soc.* **1975**, *122*, 255.
(19) Kudo, T.; Obayashi H. *J. Electrochem. Soc.* **1976**, *123*, 415.
(20) Wang, D. Y.; Nowick, A. S. *J. Solid State Chem.* **1980**, *35*, 325.
(21) Wang, D. Y.; Park, D. S.; Griffith, J.; Nowick, A. S. *Solid State Ionics* **1981**, *2*, 95.
(22) Gerhardt, R.; Nowick, A. S. *J. Am. Ceram. Soc.* **1986**, *69*, 641.
(23) Dawicke, J. W.; Blumenthal, R. N. *J. Electrochem.* Soc. **1986**, *133*, 904.
(24) Yahiro, H.; Egushi, Y.; Egushi, K.; Arai, H. *J. Appl. Electrochem.* **1988**, *18*, 527.
(25) Egushi, K.; Setoguchi, T.; Inoue, T.; Arai, H. *Solid State Ionics* **1992**, *52*, 165.
(26) De Guire, M. R.; Shingler, M. J.; Dincer, E. *Solid State Ionics* **1992**, *52*, 155.
(27) Maricle, D. L.; Swarr, T. E.; Karavolis, S. *Solid State Ionics* **1992**, *52*, 173.
(28) Tuller, H. L. *J. Phys. Chem. Solids* **1994**, *55*, 1393.
(29) Balazs, G. B.; Glass, R. S. *Solid State Ionics* **1995**, *76*, 155.

S0897-4756(97)00425-0 CCC: $14.00

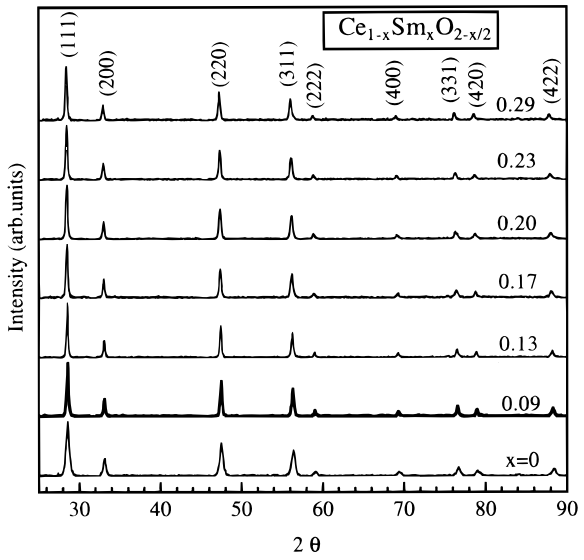

Figure 1. Powder X-ray diffraction patterns of $Ce_{1-x}Sm_xO_{2-x/2}$ solid solutions.

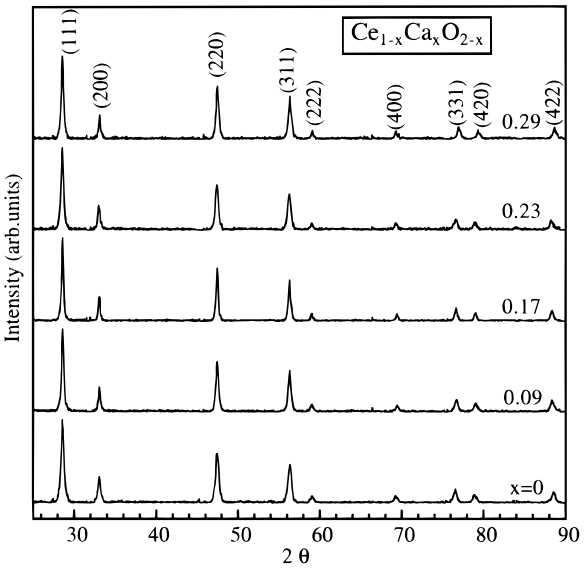

Figure 2. Powder X-ray diffraction patterns of $Ce_{1-x}Ca_xO_{2-x}$ solid solutions.

host lattice of ceria is compatible with a wide range of rare-earth ion substitutions. Among the ceria solid electrolytes, samarium-doped ceria, $Ce_{0.8}Sm_{0.2}O_{1.9}$, was found to have the highest ionic conductivity and calcium-doped ceria, $Ce_{1-x}Ca_xO_{2-x}$, has the highest conductivity among the alkaline earth substituted ceria.[2] Yttrium-doped ceria solid electrolytes have been successfully prepared by hydrothermal method, providing low-temperature preparation and morphological control in ultrafine particles of uniform crystallite dimension.[31] Recently, the properties of hydrothermally prepared $Ce_{0.8}M_{0.2}O_{1.9-y}$ (M = Sm, Ca, Sr, Gd, and Y) solid solutions have been reported.[32] A systematic study of $Ce_{1-x}M_xO_{2-y}$ and the evolution of properties of the hydrothermally prepared ceria solid solutions with increasing x has not been carried out so far.

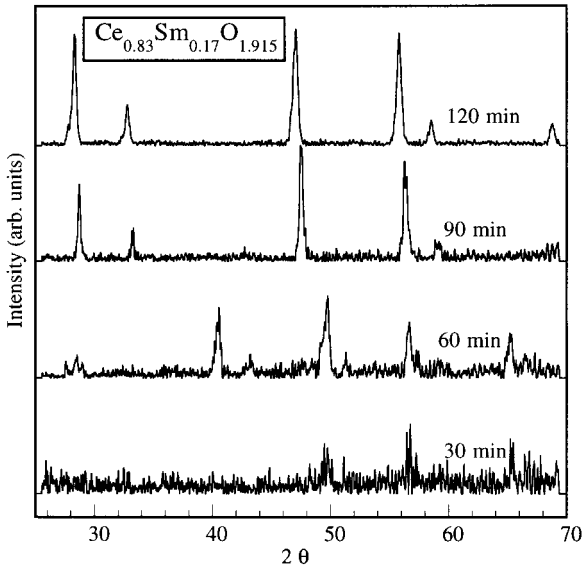

Figure 3. Powder X-ray diffraction patterns of the $Ce_{0.83}Sm_{0.17}O_{1.915}$ solid solutions quenched during hydrothermal preparation.

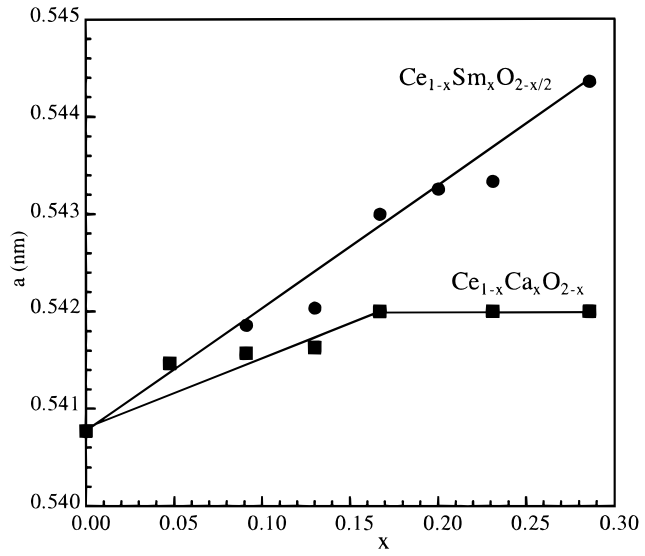

Figure 4. Lattice constants of $Ce_{1-x}Sm_xO_{2-x/2}$ and $Ce_{1-x}Ca_xO_{2-x}$ solid solutions as a function of x.

In this paper we present a systematic study of the structure, ionic conductivity, and thermophysical properties of hydrothermally prepared $Ce_{1-x}Sm_xO_{2-x/2}$ and $Ce_{1-x}Ca_xO_{2-x}$.

Experimental Section

Solid solutions $Ce_{1-x}Sm_xO_{2-x/2}$ ($x = 0-0.30$) and $Ce_{1-x}Ca_xO_{2-x}$ ($x = 0-0.30$) were synthesized by the hydrothermal method as previously reported for the limited composition of ceria solid electrolytes.[31-32] The appropriate quantities of cerium (III) nitrate hexahydrate ($Ce(NO_3)_3 \cdot 6H_2O$, 99.9% Aldrich), samarium(III) nitrate hexahydrate ($Sm(NO_3)_3 \cdot 6H_2O$, 99.9% Aldrich), or calcium nitrate hexahydrate ($Ca(NO_3)_2 \cdot 6H_2O$, 99.9% Aldrich) were dissolved separately in water, mixed, and coprecipitated with ammonium hydroxide or NaOH (1 M) at pH 10. The precipitated gels were sealed into Teflon-lined steel autoclaves and hydrothermally treated at 260 °C for several hours. The kinetics of the fluorite-phase formation was investigated during the hydrothermal synthesis. The autoclaves were quenched and the precipitated powders washed, dried, and characterized by X-ray diffraction. The crystallized powders of $Ce_{1-x}Sm_xO_{2-x/2}$ ($x = 0-0.30$) and $Ce_{1-x}Ca_xO_{2-x}$ ($x=$

(30) Christie, G. M.; Van Berkel, F. P. F. *Solid State Ionics* **1996**, *83*, 17.
(31) Zhou, Y. C.; Rahaman, M. N. *J. Mater. Res.* **1993**, *8*, 1680.
(32) Yamashita, K.; Ramanujachary, K. V.; Greenblatt, M. *Solid State Ionics* **1995**, *81*, 53.

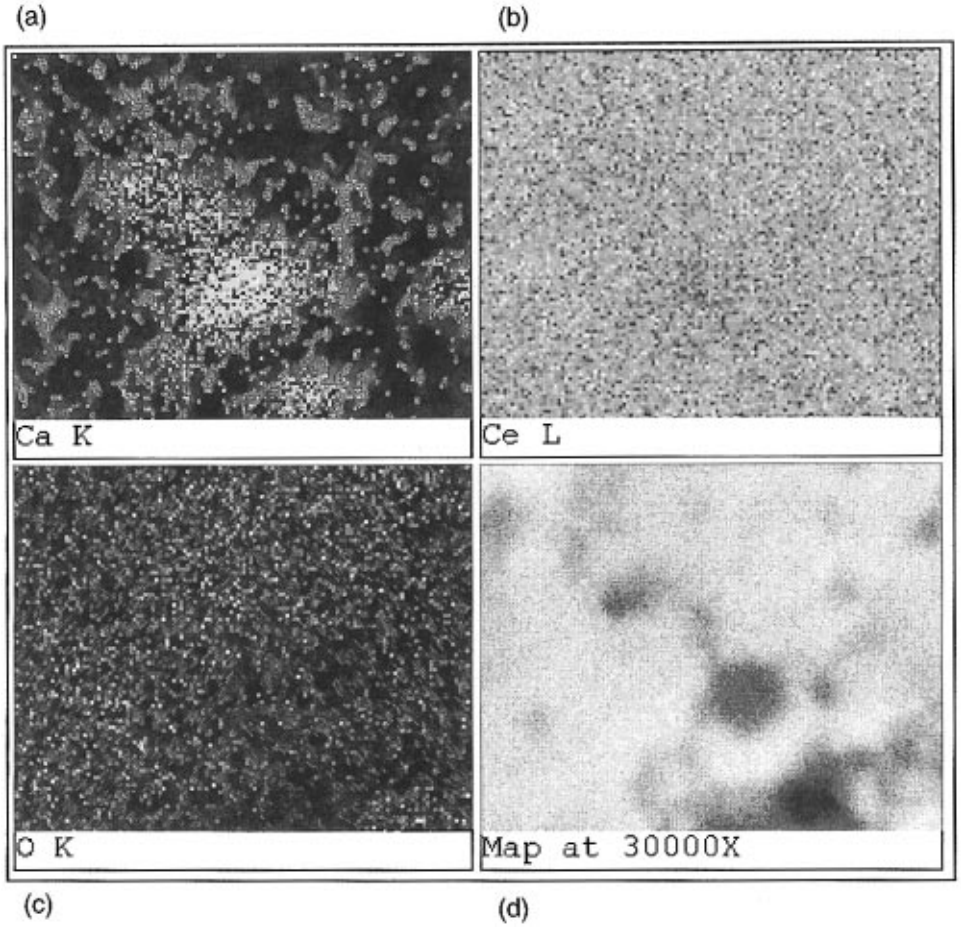

Figure 5. X-ray map of elements in a sample of $Ce_{0.71}Ca_{0.29}O_{1.71}$.

0−0.30) solid solutions were repeatedly washed with deionized water, filtered, and dried in air first at room temperature and finally at 200 °C for 2 h.

The room-/high-temperature powder X-ray diffraction patterns (PXD) of the ultrafine powders were obtained with a Scintag PAD V diffractometer equipped without/with a high-temperature attachment with monochromatized Cu Kα radiation at a 2 θ scan of 0.5 deg/min. Cell parameters were calculated by fitting the observed reflections with a least-squares program. The reflection from the (422) plane was used for the determination of average crystallite size.[31] The average crystallite size, D, of the hydrothermally prepared powders was calculated from the Scherrer formula:

$$D = 0.9\,\lambda/(\beta \cos \theta) \qquad (2)$$

where λ is the wavelength of the X-rays, θ is the diffraction angle, $\beta = (\beta_m^2 - \beta_s^2)^{1/2}$ is the corrected half-width of the observed half-width, β_m, of the (422) reflection in samples of $Ce_{1-x}Sm(Ca)_xO_{2-y}$, and β_s is the half-width of the (422) reflection in a standard sample of CeO_2 ($D \sim 100$ nm). Differential thermal analysis (DTA) and thermogravimetric analysis (TGA) measurements were carried out in the temperature range 25−750 °C with a TA Instruments DSC 2910 and TGA 2050 with a heating and cooling rate of 2 °C/min.

The powder samples were pelletized and sintered at 1400−1450 °C for 10 h with a programmed heating and cooling rate of 5 °C/min. The sintered samples were over 95% of the theoretical density in all cases. The microstructure of sintered samples was studied using the field emission scanning electron microscope (FESEM, Model DSM 962, Gemini, Carl Zeiss, Inc., Germany) equipped with an energy-dispersive spectroscopy system (EDS, Princeton, Gamma Tech Inc., NJ) for semiquantitative analysis of Ce, Sm, or Ca. The electrical conductivity of the materials was measured on a sintered ceramic pellet. Silver paste was painted onto two faces of the pellets, using GC Electronics paste. The sample was then dried and fired at 650 °C. The ionic conductivity measurements were performed by the complex impedance method at frequencies ranging from 0.1 Hz to 20 kHz (Solartron 1280 frequency response analyzer) on isothermal plateaus 1 h long, in air on heating and cooling every 25−50 °C up to 650 °C.

Results and Discussion

The PXD data in Figures 1 and 2 show that $Ce_{1-x}Sm_xO_{2-x/2}$ and $Ce_{1-x}Ca_xO_{2-x}$, prepared by the hydrothermal synthesis for the first time in a relatively wide concentration range, form solid solutions with the fluorite structure in the investigated range $x = 0-0.30$ for Sm substitution in good agreement with our results by sol−gel method,[33] and in the range $x = 0-0.17$ for Ca substitution. The fluorite-phase evolution during the hydrothermal process examined by PXD for $Ce_{0.83}Sm_{0.17}O_{1.915}$ is shown in Figure 3. Each sample was prepared under the same condition and heated in an autoclave at 260 °C for various periods as indicated in Figure 3. At the end of designated heating time, the sample was quenched, dried, and characterized by PXD. After 30 min, the precipitated product is a gray amorphous multiphase. When the autoclave is in the furnace at 260 °C for ∼1 h, broad peaks are seen in the PXD (Figure 3), which correspond primarily to the intermediate phase of cerium/samarium hydroxide ($Ce/Sm(OH)_3$). After the sample is heated for 90 min, the PXD is that of pure CeO_2. Further heat treatment to 120 min improves the crystallinity of the sample. The unit cell

(33) Huang, W.; Shuk, P.; Greenblatt, M. *Solid State Ionics*, in press.

Table 1. Lattice Parameters (a), Average Crystallite Sizes (D), and Electrical Properties[a] of $Ce_{1-x}Sm_xO_{2-x/2}$ and $Ce_{1-x}Ca_xO_{2-x}$ Solid Solutions

composition $Ce_{1-x}Sm(Ca)_xO_{2-y}$	a (nm)	D (nm)	$\sigma_{600\ °C}$ (S/cm) (±10%)	E_a (eV)
Sm				
$x = 0$	0.54077 (2)	50	1.1×10^{-5}	1.03
$x = 0.09$	0.54186 (8)	68	9.8×10^{-4}	0.80
$x = 0.13$	0.54204 (5)	68	1.3×10^{-3}	0.88
$x = 0.17$	0.54300 (7)	50	5.7×10^{-3}	0.92
$x = 0.20$	0.54326 (6)	40	2.0×10^{-3}	0.87
$x = 0.23$	0.54334 (7)	50	1.4×10^{-3}	1.04
$x = 0.29$	0.54436 (3)	68	6.2×10^{-4}	1.03
Ca				
$x = 0.05$	0.54147 (6)	40	1.4×10^{-3}	0.93
$x = 0.09$	0.54157 (5)	40	2.1×10^{-3}	0.83
$x = 0.17$	0.54200 (4)	50	1.5×10^{-3}	0.81
$x = 0.23$	0.54203 (6)	50	4.2×10^{-4}	0.93

[a] Conductivity, σ. Activation energy, E_a.

parameter a increases linearly with increasing Sm and Ca content as expected from effective ionic radii ($r_{Ce^{4+}} = 0.1110$ nm; $r_{Sm^{3+}} = 0.1219$ nm; $r_{Ca^{2+}} = 0.1260$ nm) considerations.[34] Figure 4 suggests that the solubility limit of Ca is $x = 0.17$. This value is significantly lower than $x = 0.23$ as determined by high temperature solid-state reaction.[35] It is noteworthy that the PXD of phases with x up to 0.29 prepared here show no evidence of impurity (Figure 2); nevertheless, the unit cell parameter remains constant for $x > 0.17$. The X-ray map of elements on the sample with nominal composition $Ce_{0.71}Ca_{0.29}O_{1.71}$ (Figure 5a−d) from EDS shows clear nonhomogeneity of Ca in the sample in Figure 5a. The excess of unincorporated CaO shows up as an amorphous phase at the grain boundaries or on the grain surface (dark region in Figure 5d). The average crystallite sizes of both the samarium- and calcium-substituted ceria powders, after drying at 200 °C, calculated by the Scherrer formula from the PXD data were between 40 and 68 nm (Table 1). The fine samarium- and calcium-substituted ceria powders were sintered into pellets with apparent densities over 95% of the theoretical value even at 1400 °C, whereas $Ce_{1-x}Sm(Ca)_xO_{2-y}$, prepared by conventional ceramic techniques, requires over 1600 °C for sintering. The SEM micrographs of ceria samples sintered at 1400 °C in Figure 6 indicate relatively small particles of ∼100−500 nm and that the microstructure is relatively dense. As expected, these particles are considerably larger than those of the "as-prepared" powder. Temperature dependent X-ray measurements show that the lattice constant increases linearly with temperature (Figure 7); the thermal expansion coefficients determined from these data are 8.6×10^{-6} and 9.4×10^{-6} K^{-1} for the $Ce_{0.83}Sm_{0.17}O_{1.915}$ and $Ce_{0.91}Ca_{0.09}O_{1.91}$, respectively.

Pure ceria oxide is basically a poor oxide ion conductor ($\sigma_{600\ °C} \sim 10^{-5}$ S/cm). The ionic conductivities were significantly enchanced in $Ce_{1-x}Sm_xO_{2-x/2}$ and $Ce_{1-x}Ca_xO_{2-x}$ solid electrolytes by increasing the oxygen vacancies ($V_O^{\bullet\bullet}$). The ionic conductivity of $Ce_{1-x}Sm_xO_{2-x/2}$ increases systematically with increasing samarium substitution and reaches a maximum at $x = 0.17$ (Figure 8). As noted before,[33] the decrease in the ionic conductivity for higher x (in our case for $x > 0.17$) is ascribed

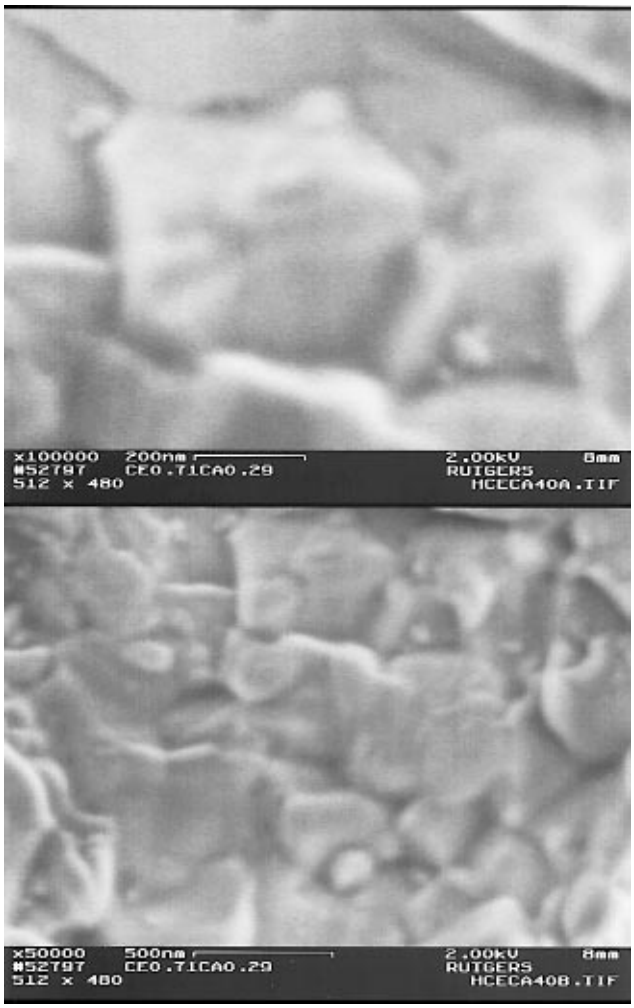

Figure 6. Scanning electron microscope photograph of the surface of densified (i.e., annealed at 1400 °C for 4 h) $Ce_{0.71}Ca_{0.29}O_{1.71}$.

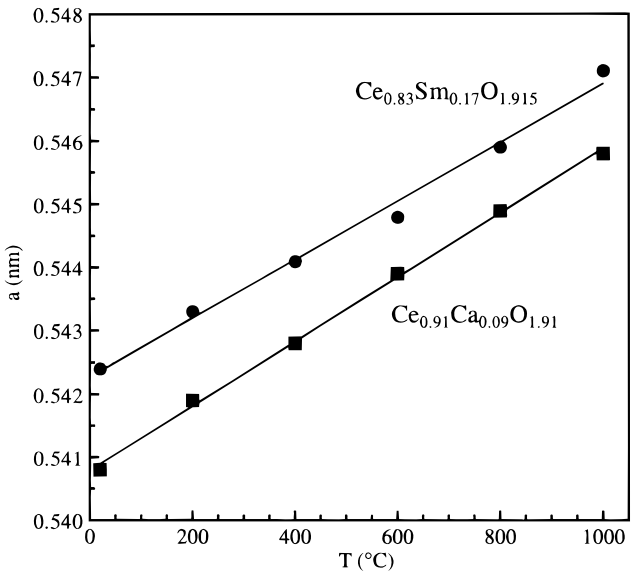

Figure 7. Temperature dependence of the lattice constants of selected ceria solid electrolytes.

to defect associations of the type $\{Sm_{Ce}'V_O^{\bullet\bullet}\}$ at higher concentrations of $V_O^{\bullet\bullet}$. In the $Ce_{1-x}Ca_xO_{2-x}$ system, Ca substitution introduces twice the number of oxygen vacancies as that of Sm substitution for the same value of x, and the ionic conductivity reaches a maximum

(34) Shannon, R. D.; Prewitt, C. T. *Acta Crystallogr.* **1976**, *32A*, 751.
(35) Yahiro, H.; Ohuchi, T.; Egushi, K.; Arai, H. *J. Mater. Sci.* **1988**, *23*, 1036.

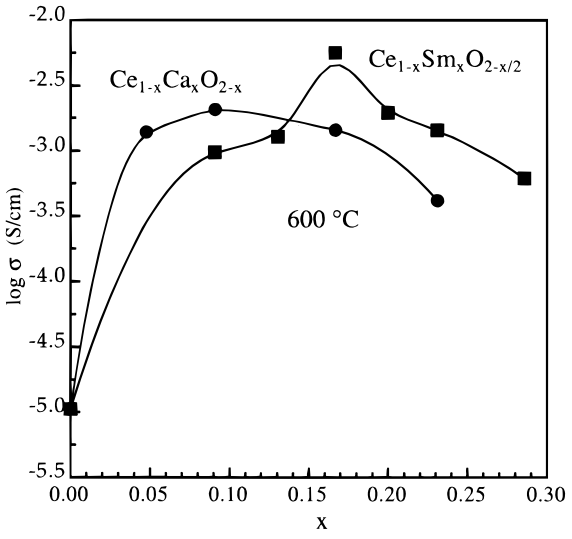

Figure 8. Concentration dependence of the ionic conductivity of $Ce_{1-x}Sm_xO_{2-x/2}$ and $Ce_{1-x}Ca_xO_{2-x}$ solid solutions.

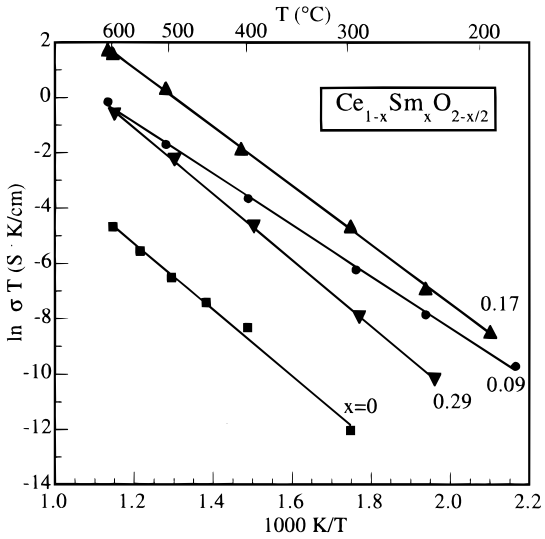

Figure 9. Arrhenius plots of the ionic conductivity of $Ce_{1-x}Sm_xO_{2-x/2}$ solid solutions.

already at $x = 0.09$. Again, the conductivity decreases for $x > 0.09$ due to the formation of complex defect associations $\{Ca_{Ce}''V_O^{\bullet\bullet}\}$. Linear Arrhenius plots, $\ln(\sigma T) = \ln A - E_a/kT$, over a wide temperature range (Figures 9 and 10) indicate the presence of only one mode of oxide ion conduction in the substitution range of both Sm and Ca.

The migration enthalpy (ΔH_m) for oxide anions through the ceria lattice is dependent upon both the oxygen binding energy in the lattice and the "free volume" through which the oxide ions migrate; i.e., ΔH_m consists of the energy required to break a lattice cation−oxygen bond and the energy term dependent on oxide ion mobility between vacant lattice sites.[36,37] The average M−O binding energy in the lattice [ABE = $(1 - x)$BE-(Ce−O) + xBE(Ca/Sm−O)] obtained from the Born−Haber cycle,[37] decreases linearly with increasing dopant content of Sm^{3+} or Ca^{2+}. The free volume, defined as the difference between the ceria unit cell volume (as calculated from the unit cell parameters) and the total

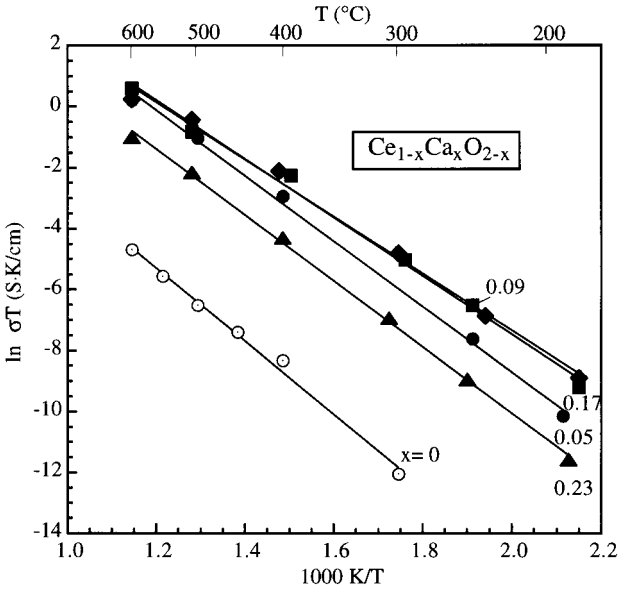

Figure 10. Arrhenius plots of the ionic conductivity of $Ce_{1-x}Ca_xO_{2-x/2}$ solid solutions.

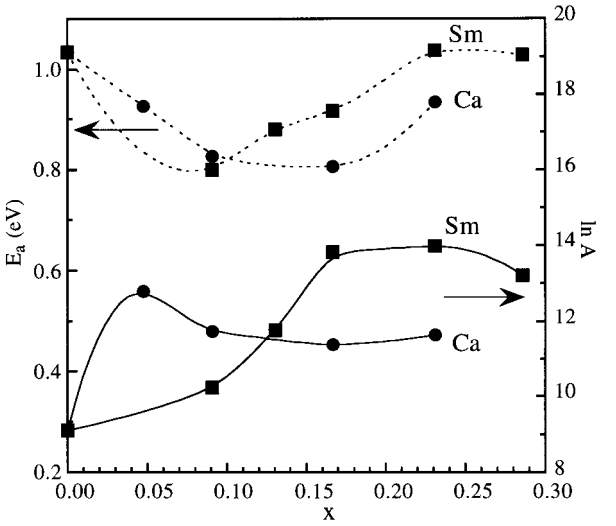

Figure 11. Dependence of activation enthalpy, E_a, and preexponential factor, A, in the Arrhenius equation on Sm- or Ca-dopant concentration in $Ce_{1-x}Sm_xO_{2-x/2}$ and $Ce_{1-x}Ca_xO_{2-x}$ solid solutions.

volume occupied by all the ions present within the unit cell (calculated from the effective ionic radii), tends to increase with increasing Sm or Ca substitutions and it is larger for $Ce_{1-x}Sm_xO_{2-x/2}$. Consistent with these results, the oxide ion conductivity of $Ce_{1-x}Sm_xO_{2-x/2}$ or $Ce_{1-x}Ca_xO_{2-x}$ solid electrolytes increases with Sm or Ca substitution up to a maximum at $x = 0.17$ or $x = 0.09$, respectively. Above the maximum value of x the defect associations $\{Sm_{Ce}'V_O^{\bullet\bullet}\}$ or $\{Ca_{Ce}''V_O^{\bullet\bullet}\}$ lead to decrease of oxygen vacancies and the ionic conductivity. In both systems the activation enthalpy for oxide ion conductivity, E_a, and the preexponential factor, A, reached a minimum and a maximum (Figure 11), respectively, at the Sm/Ca content, just before the complex formation [$\{Sm_{Ce}'V_O^{\bullet\bullet}\}$ or $\{Ca_{Ce}''V_O^{\bullet\bullet}\}$] begins to dominate. The highest ionic conductivity found for the $Ce_{0.83}Sm_{0.17}O_{1.915}$ composition, $\sigma_{600\ °C} \sim 6 \times 10^{-3}$ S/cm, is identical with that previously found by Balazs and Glass ($\sigma_{600\ °C} \sim 10^{-2}$ S/cm),[29] prepared by solid-state reaction, and our results for sol−gel prepared $Ce_{0.80}Sm_{0.20}O_{1.9}$.[33]

(36) Cook, R. L.; MacDuff, R. C.; Sammells, A. F. *J. Electrochem. Soc.* **1990**, *137*, 3309.
(37) Cook, R. L.; Sammells, A. F. *Solid State Ionics* **1991**, *45*, 311.

Conclusion

$Ce_{1-x}Sm_xO_{2-x/2}$ ($x = 0-0.30$) and $Ce_{1-x}Ca_xO_{2-x}$ ($x = 0-0.17$) solid solutions with the fluorite structure were prepared in <2 h at 260 °C by the hydrothermal method. Ultrafine particles of uniform crystallite dimension ~40−68 nm formed. Because of the small particle size of the ceria, the sintering temperature needed to obtain a dense ceramic pellet was reduced substantially from 1600 °C, that required for the corresponding materials prepared by conventional solid-state methods, to ~1400 °C. The maximum ionic conductivity was found for the $x = 0.17$ Sm and $x = 0.09$ Ca substituted ceria ($\sigma_{600\ °C} = 5.7 \times 10^{-3}$ S/cm, $E_a \approx 0.9$ eV and $\sigma_{600\ °C} = 2.1 \times 10^{-3}$ S/cm, $E_a \approx 0.8$ eV, respectively). The thermal expansion coefficients, determined from high-temperature X-ray data, are 8.6×10^{-6} and 9.4×10^{-6} K^{-1} for the best conducting $Ce_{0.83}Sm_{0.17}O_{1.915}$ and $Ce_{0.91}Ca_{0.09}O_{1.91}$ solid electrolytes, respectively.

CM970425T